Systematic Effects on the Estimation of the H_0 with Gravitational Waves

Author: Pablo Miguel Cifuentes Espitia
Advisor: Antonio Enea Romano
Grupo : Cosmograv, udea
Universidad de Antioquia
Facultad de Ciencias Exactas y Naturales
Instituto de Física

The Content

1. Introduction
2. The Hubble tension
3. Theoretical framework
4. Mock data challenge
5. Conclusions

UNIVERSIDAD
DE ANTIOQUIA
1 8 0 3

The Content

1. Introduction

UNIVERSIDAD DE ANTIOQUIA
1 8 0 3

Compact Binary Systems

A compact binary system is composed of two compact stellar objects, such as a Binary system of two Neutron Stars (BNS) or Binary system of two Black Holes (BBH) or a mixture of a Neutron Star (NS) and a Black Hole (BH) orbiting around each other.

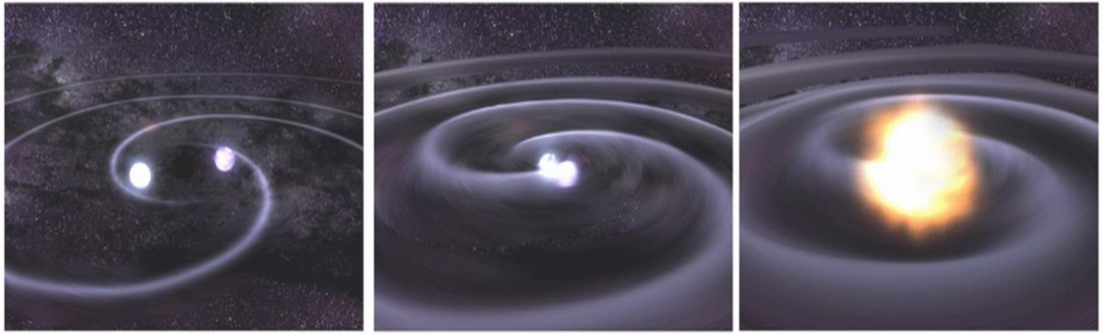

NASA/CXC/GSFC/T.Strohmayer

International Network of Gravitational-Wave Detectors

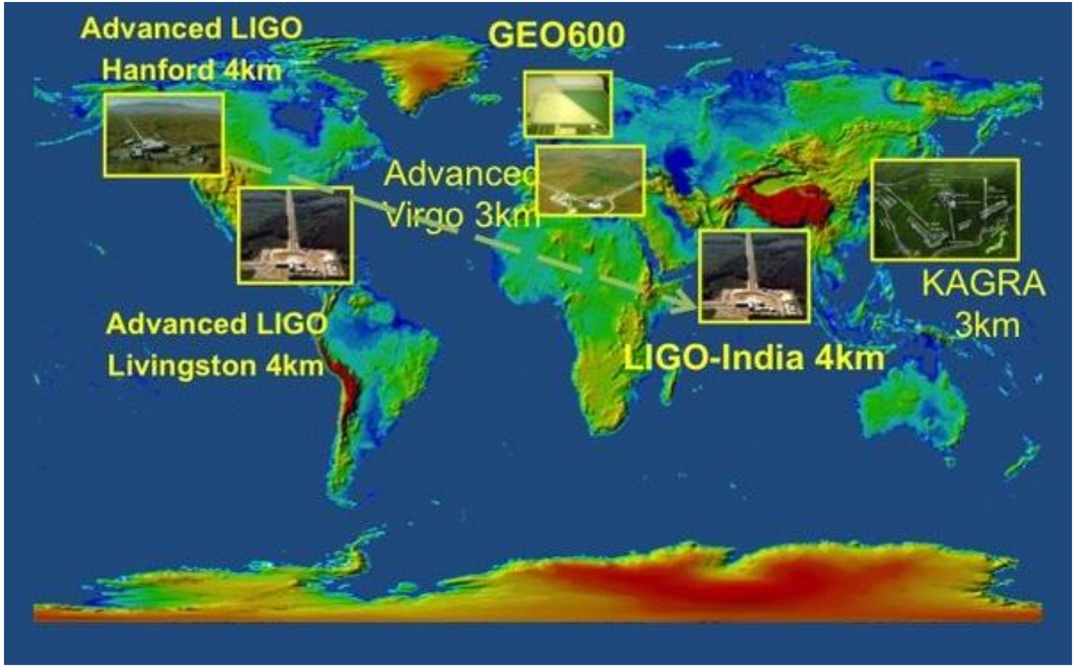

https://www.nature.com/articles/nindia.2016.20

The two LIGO detectors

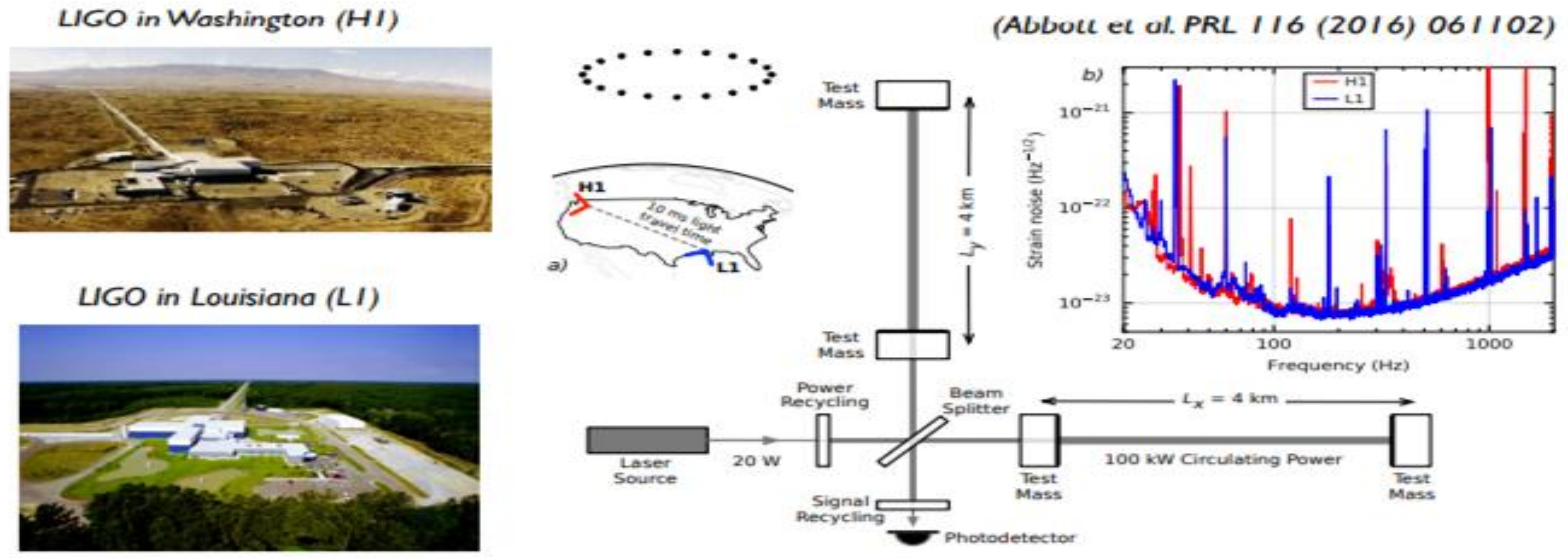

https://www.ligo.caltech.edu/page/ligo-detectors

LIGO detections during O1

(Abbott et al. PRL 116 (2016) 061102)

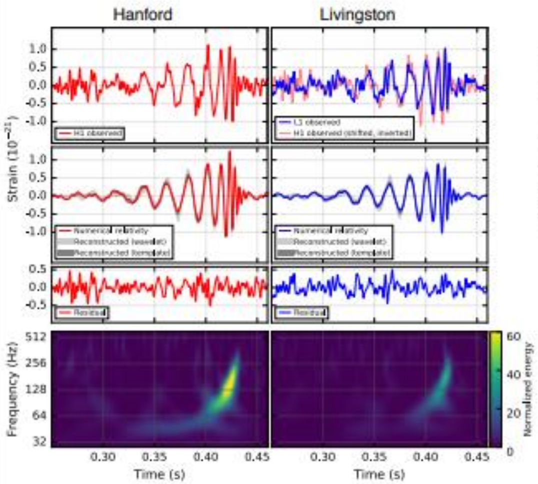

(Abbott et al. PRL 116 (2016) 241103)

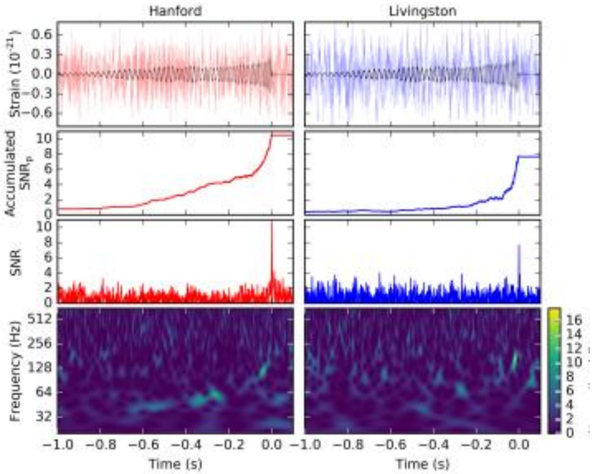

- **GW150914**: SNR=24 (very loud), 10 GW cycles, **0.2 sec.**
- **GW151226**: SNR=13 (quieter), 55 GW cycles, **1.5 sec.**

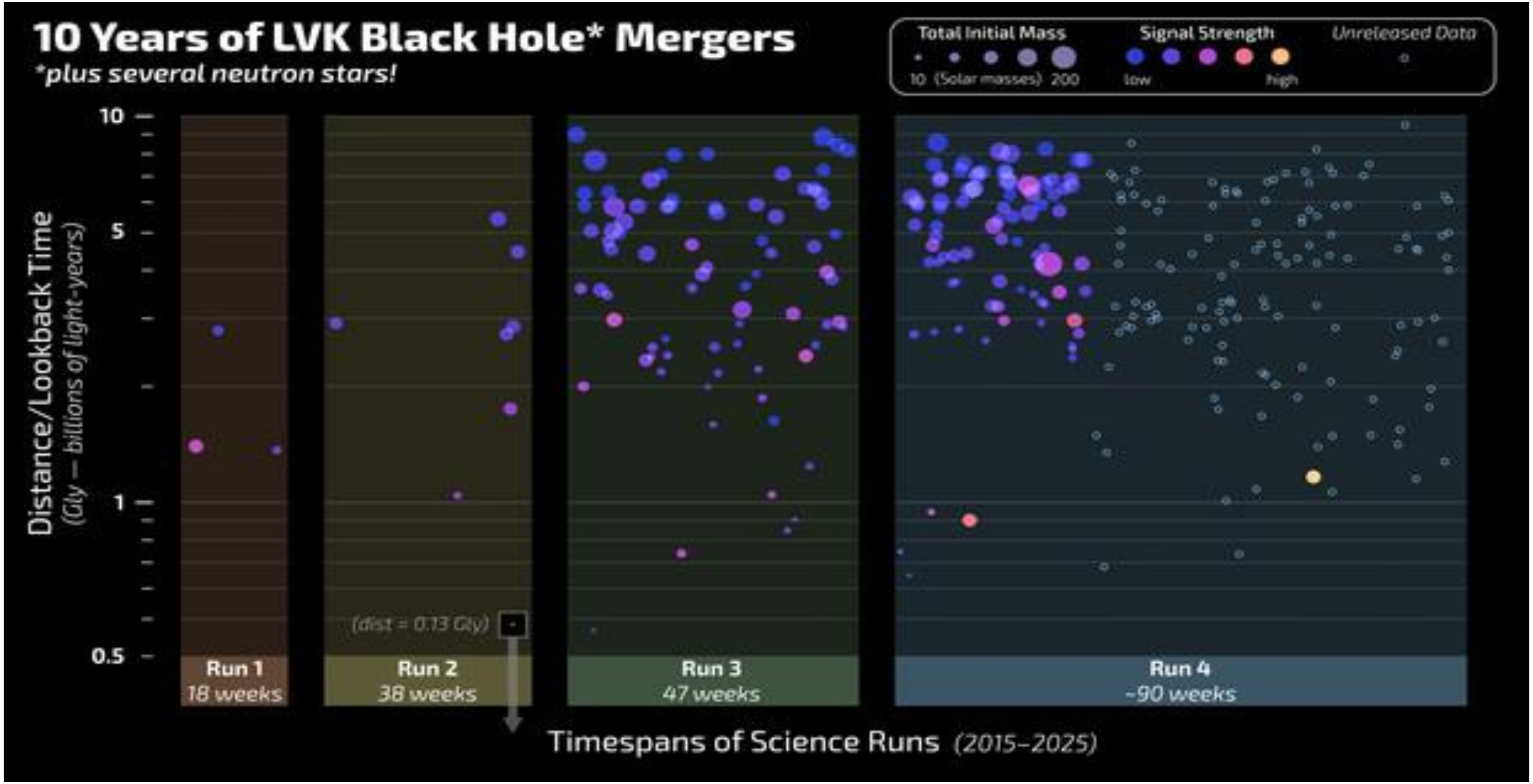

https://www.ligo.caltech.edu/image/ligo20250910b

The Content

1. Introduction
2. The Hubble tension

UNIVERSIDAD
DE ANTIOQUIA
1 8 0 3

The Hubble tension

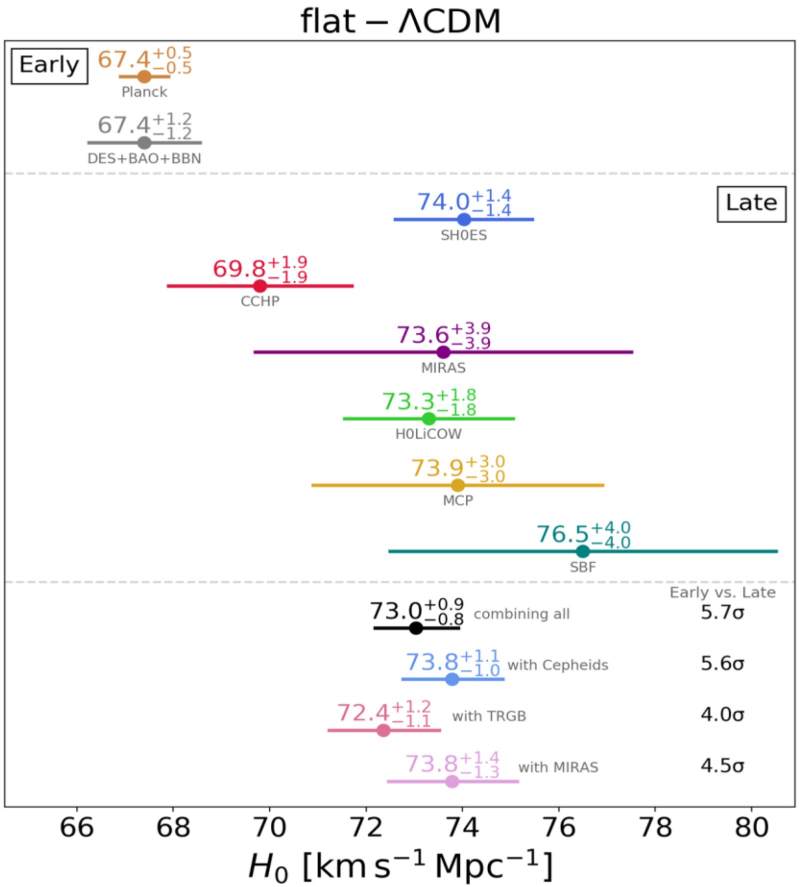

UNIVERSIDAD DE ANTIOQUIA
1 8 0 3

https://github.com/ vbonvin/H0_tension.

The Content

1. Introduction
2. The Hubble tension
3. Theoretical framework

UNIVERSIDAD
DE ANTIOQUIA
1 8 0 3

Bayesian Framework

$$p(\theta|d) = \frac{\mathcal{L}(d|\theta)\pi(\theta)}{\mathcal{Z}},$$

$$\mathcal{Z} = \int d\theta \mathcal{L}(d|\theta)\pi(\theta).$$

https://arxiv.org/abs/2502.00239

UNIVERSIDAD DE ANTIOQUIA
1 8 0 3

Bayesian Framework

The detection rate for the analysis of dark sirens

$$\mathcal{L}(x \mid \Lambda) \propto \frac{\sum_{i=1}^{N_{\rm obs}} \int \mathcal{L}(x_i \mid \theta, \Lambda) \frac{dN}{dt\, d\theta} d\theta}{\int p_{\rm det}(\theta, \Lambda) \frac{dN}{dt\, d\theta} d\theta}.$$

https://arxiv.org/abs/2305.17973

UNIVERSIDAD DE ANTIOQUIA
1 8 0 3

Bayesian Framework

$$\mathcal{L}(x \mid \Lambda) \propto \frac{\sum_{i=1}^{N_{\rm obs}} \int \mathcal{L}(x_i \mid \theta, \Lambda) \frac{dN}{dt\, d\theta} d\theta}{\int p_{\rm det}(\theta, \Lambda) \frac{dN}{dt\, d\theta} d\theta}.$$

$$\frac{dN}{d\theta_D\, dt_d} = \frac{dN}{d\theta_S\, dt_S} \frac{dt_S}{dt_d} \frac{1}{\det(J_{D\to S})} = \frac{dN}{d\theta_S\, dt_S} \frac{1}{1+z} \frac{1}{\det(J_{D\to S})},$$

https://arxiv.org/abs/2305.17973

UNIVERSIDAD DE ANTIOQUIA 1803

Bayesian Framework

$$\frac{dN}{d\theta_D\, dt_d} = \frac{dN}{d\theta_S\, dt_S}\frac{dt_S}{dt_d}\frac{1}{\det(J_{D\to S})} = \frac{dN}{d\theta_S\, dt_S}\frac{1}{1+z}\frac{1}{\det(J_{D\to S})},$$

The detection rate for the analysis of dark sirens is parameterized as follows:

$$\frac{dN}{d_L\, dm_{1,d}\, dm_{2,d}\, d\chi\, dt_d} = R_0\Psi(z;\Lambda)\times p_{\mathrm{pop}}(m_{1,s}, m_{2,s} \mid \Lambda)p_{\mathrm{pop}}(\chi \mid \Lambda)\frac{dV_c}{dz}\frac{1}{1+z}\frac{1}{\det(J_{D\to S})},$$

$$\det(J_{D\to S}) = \frac{\partial d_L}{\partial z}(1+z)^2,$$

UNIVERSIDAD DE ANTIOQUIA 1803

https://arxiv.org/abs/2305.17973

Luminosity distance in ΛCDM

$$d_L(z) = \frac{c(1+z)}{H_0}\int_0^z \frac{H_0}{H(z')}dz',$$

https://arxiv.org/abs/1807.03098

UNIVERSIDAD DE ANTIOQUIA
1 8 0 3

At low redshifts z ≪ 1

$$d_L(z) = \frac{c(1+z)}{H_0} \int_0^z \frac{H_0}{H(z')} dz',$$

↓

$$d_L(z) \approx cz/H_0,$$

https://arxiv.org/abs/1807.03098

UNIVERSIDAD DE ANTIOQUIA 1803

At low redshifts z ≪ 1

$$d_L(z) = \frac{c(1+z)}{H_0} \int_0^z \frac{H_0}{H(z')} dz',$$

$$d_L(z) \approx cz/H_0,$$

https://arxiv.org/abs/1807.03098

UNIVERSIDAD DE ANTIOQUIA
1803

Gravitational waves

The distortion of a gravitational wave signal depends on the intrinsic properties of the source and its orientation relative to the location where the measurement is performed.

$$h_+ \equiv \frac{2M}{d_L}(1+\cos^2 i)(\pi \mathcal{M}_c f)^{2/3}\cos(\Phi+\Psi),$$

$$h_\times \equiv \frac{4M}{d_L}\cos i(\pi \mathcal{M}_c f)^{2/3}\sin(\Phi+\Psi),$$

https://arxiv.org/abs/gr-qc/9301003

UNIVERSIDAD DE ANTIOQUIA
1803

Gravitational waves

The distortion of a gravitational wave signal depends on the intrinsic properties of the source and its orientation relative to the location where the measurement is performed.

$$h_+ \equiv \frac{2M}{d_L}(1+\cos^2 i)(\pi \mathcal{M}_c f)^{2/3}\cos(\Phi+\Psi),$$

$$h_\times \equiv \frac{4M}{d_L}\cos i(\pi \mathcal{M}_c f)^{2/3}\sin(\Phi+\Psi),$$

https://arxiv.org/abs/gr-qc/9301003

UNIVERSIDAD DE ANTIOQUIA
1 8 0 3

The Content

1. Introduction
2. The Hubble tension
3. Theoretical framework
4. Mock data challenge

UNIVERSIDAD
DE ANTIOQUIA
1 8 0 3

Mock Data Challenge

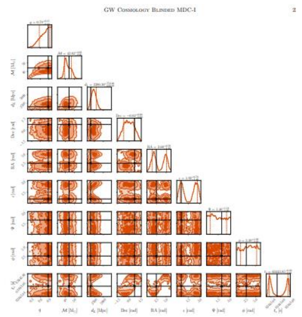

DATA SIMULATED

PRIORS

POSTERIOR

ICAROGW: A python package for inference of astrophysical population properties of noisy, heterogeneous and incomplete observations

UNIVERSIDAD DE ANTIOQUIA
1803

https://arxiv.org/abs/2305.17973

Results from the Blinded-MDC

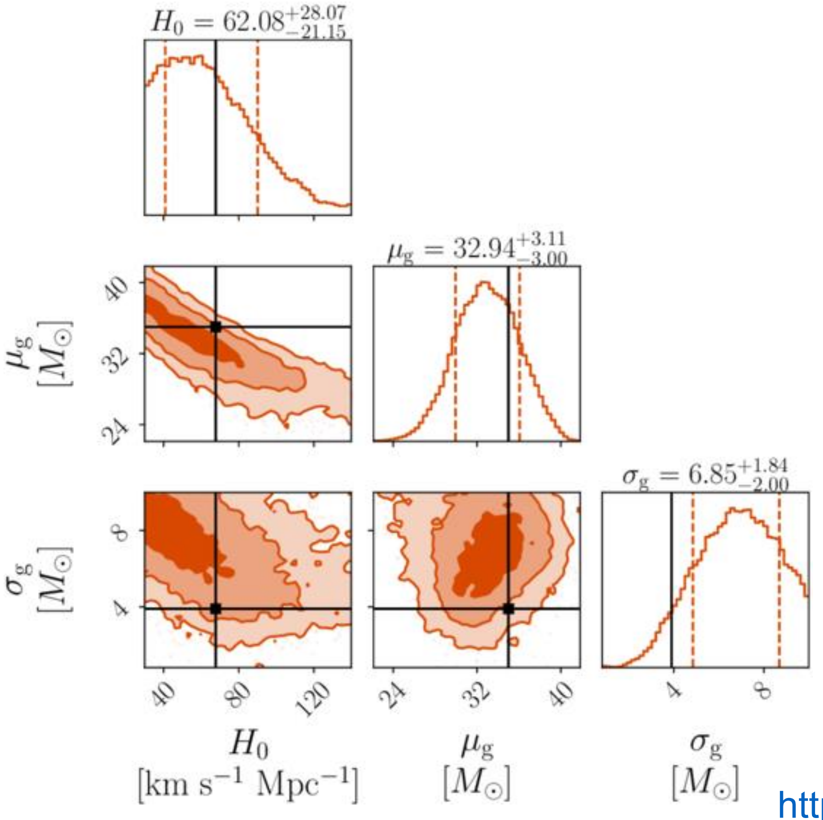

Vanilla Model Results

UNIVERSIDAD DE ANTIOQUIA
1 8 0 3

https://arxiv.org/abs/2412.14244

Results from the Blinded-MDC

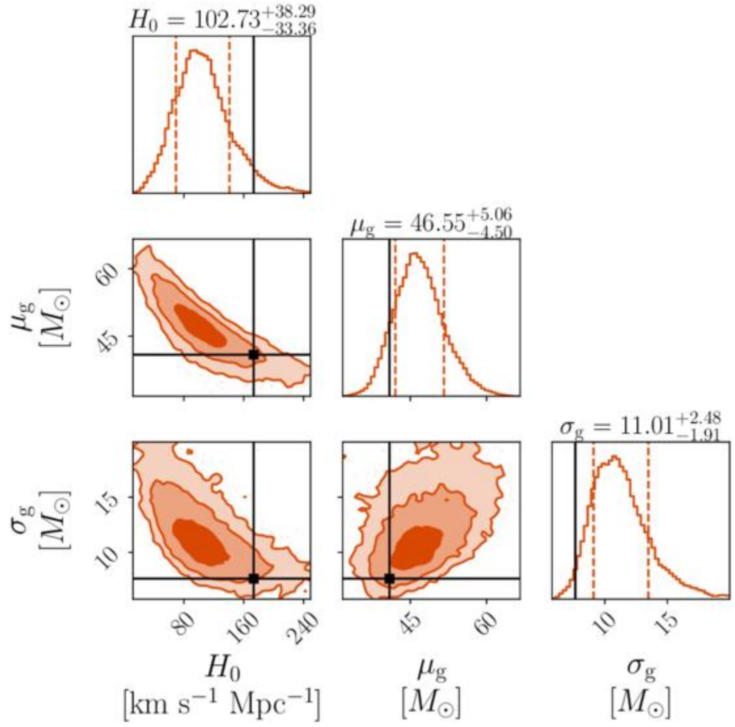

Redshift-dependent Scenario Results

UNIVERSIDAD DE ANTIOQUIA
1 8 0 3

https://arxiv.org/abs/2412.14244

The Content

1. Introduction
2. The Hubble tension
3. Theoretical framework
4. Mock data challenge
5. Conclusions

UNIVERSIDAD
DE ANTIOQUIA
1803

Conclusions

- The **Simulated Data Challenge with hidden parameters** shows that although ICAROGW proves effective under ideal conditions and models consistent with the simulation process, its performance may degrade in the presence of structural discrepancies between simulation and analysis.
- This limitation highlights the importance of carefully considering **population evolution as a function of redshift** in future inference campaigns, especially when aiming to measure cosmological parameters with high precision.

Thanks

UNIVERSIDAD DE ANTIOQUIA
1803